Strangeness production in proton and heavy-ion collisions at 14.6 A GeV

N. S. Amelin, E. F. Staubo, and L. P. Csernai
Physics Department, University of Bergen, Allegaten 55, N-5007 Bergen, Norway

V. D. Toneev and K. K. Gudima
Joint Institute for Nuclear Research, Theoretical Physics Laboratory, Dubna, U.S.S.R.
(Received 10 May 1991)

Rapidity and transverse momentum distributions of π^-, $K^\pm$, and p have been computed for $p+$Be, $p+$Au, and Si+Au collisions at 14.6 A GeV with the Monte Carlo quark-gluon string model (QGSM). The calculations are compared to experimental data at the same energy. The QGSM reproduced the shapes and approximately absolute values of the minimum bias rapidity distribution for all particles except the pions in $p+$Au data. The model also reproduced the rapidity distribution for protons and K^+ in the central Si+Au collisions. However, we overestimated the enhancement at low p_t for pions and negative kaons. As a consequence, the QGSM also produces an excess of pions and K^- in the rapidity distribution below $y=2$, and predicted an overall K^+/π^+ enhancement by a factor of 1.4–1.9 as compared to pp data, instead of a factor of 4 as obtained by the E802 Collaboration.

I. INTRODUCTION

Heavy-ion experiments at relativistic and at ultrarelativistic energies have largely been motivated by the search for a quark-gluon plasma (QGP), a macroscopic state of matter where quarks and gluons are free to move in a large volume. At Brookhaven National Laboratory–Alternating Gradient Syncrotron (AGS), full stopping is realized [1–4], showing a behavior close to the Landau model [5] and to relativistic fluid dynamics [6], and the energy density can reach values comparable to the critical values for QGP formation. At CERN-SPS energies, the situation is rather different: the projectile and target would penetrate through each other, and the nucleus becomes more transparent. However, different CERN experiments (NA35, WA80) demonstrate a substantial stopping power (60%, NA35), and estimates from particle production density (WA80) indicate energy densities above critical values.

Monte Carlo quark-gluon string model (QGSM) calculations agree well with transverse energy spectra observed at AGS energies [7,8] and for CERN-SPS energies [9,10], the QGSM also predicts a high level of collectively and thermalization for heavy systems and even observable transverse flow for Pb+Pb reactions [10].

Several observables have been proposed as signals for QGP formation, such as strangeness enhancement, dilepton production, direct photons, J/ψ suppression, and others, which probe different stages of the reaction [11–14]. A series of experiments has recently been performed to investigate strangeness enhancement. The collaborations NA35 and WA85 at SPS-CERN and E802 at AGS-BNL all claim to see an increased strangeness production as compared to $p+p$ data. But they all have to be carefully examined before specific conclusions can be made.

In order to make detailed predictions for the case of purely hadronic matter, we will analyze these experiments with the QGSM [15–18]. In this article we present rapidity and transverse momentum distributions of protons, pions, and kaons in $p+$Be, $p+$Au, and Si+Au collisions at 14.6 A GeV and compare our calculations to E802 [19,20] and E810 [21] AGS-BNL experiments. We present also K^+/π^+ and K^-/π^- ratios, predicted by the QGSM as a function of impact parameter in Si+Au at 14.6 A GeV.

II. MONTE CARLO QUARK-GLUON STRING MODEL

The QGSM is a detailed, realistic microscopic model [15–18] based on string phenomenology which does not assume QGP formation. In hadron–hadron ($h+h$), hadron-nucleus ($h+A$), and nucleus-nucleus ($A+A$) collisions, one or more strings are formed, which later decay via secondary-hadron formation. The parameters of the model were adjusted to known $h+h$ and $h+A$ data. In the QGSM the string decay product can rescatter. Another important new physical feature is the interaction of strings (treated in an approximate way by allowing the diquarks in a string, which have not yet hadronized, to rescatter). There are other models which also include similar features such as VENUS by Werner [22] and relativistic molecular dynamics (RQMD) by Sorge and coworkers [23,24].

At low incident energies, when strings have a short lifetime or the initial energy is not enough to create strings, our model can be regarded as an extension of the intranuclear cascade model [25], where we have taken into account the resonance creation, interaction, and decay, as well as direct meson creation such as $NN \rightarrow \pi NN$. During a nucleus-nucleus collisions at ultrarelativistic energies, the different kinds of hadrons can be produced. The new hadrons can interact with each other. Our mod-

el for hadron-hadron inelastic interaction is quarkbased; thus we can simulate any hadron collision in a similar manner [18]. To compute the statistical weights for the different subprocesses and to determine the interaction between hadrons, we used the experimental total, elastic, and annihilation cross sections.

For lack of experimental cross sections, we invoke isotopic invariance or additive quark model relations (for example, to compute the meson-meson collision cross sections). The resonance cross sections are assumed to be identical to the stable particle cross sections with the same quark content. An exception was made for the Δ resonance nucleon cross sections at low initial momentum, where we used the one-pion-exchange model as was described in Ref. [26]. We have also used the detailed balance relations to separate the $\Delta N \rightarrow NN$ reaction cross section and have taken into account Δ resonance production from pion and nucleon and the vector-meson production from two mesons. The probability for Δ production is determined from the relativistic Breit-Wigner distribution [26]. Delta production and the reaction $\Delta N \rightarrow NN$ are the main processes for the pion absorption inside a nucleus in the QGSM.

The QGSM has several possibilities to account for strangeness production and transverse momentum distributions. The strange particles are produced by decay of strings with strange and nonstrange quarks at their ends. The production rate is determined by the strange quark content of the colliding hadrons and by the strangeness suppression probability at string breakup. Few-particle reactions of hadrons are particularly important for strangeness production and absorption at 14.6A GeV. The details of the model are described in [18] where one can find comparisons of calculated partial cross sections for nonstrange and strange particle production in pp and $\bar{p}p$ at laboratory projectile energy around 1–10 GeV. The good agreement obtained for these processes was also obtained for meson-nucleon partial cross sections. This is illustrated by the partial cross sections for $K^{\pm}p$ reactions in Fig. 1.

The transverse distribution is essentially governed by the quark transverse distribution

$$f_t(p_t)=f_0 e^{-\beta p_t^2},$$

where f_0 and β corresponding, respectively, to the normalization constant and to a slope parameter. They are different in cases of string breaking and intrinsic quark transverse momentum, $\beta=6.25$ and 8.2 $(\mathrm{GeV}/c)^{-2}$, respectively [27]. An additional source of transverse momentum creation arises from rescattering of the secondaries or rescattering of the leading diquarks of the strings which have not yet hadronized completely. Finally, a further source of the transverse momentum is the original transverse Fermi motion of the nucleons in the projectile and target. This transverse motion is inherited by the valence quarks and diquarks. Hence the original strings formed by the valence quarks or diquarks of the initial projectile and target nucleons are not completely parallel to the beam axis.

It should be mentioned that for the AGS energy most of the strings have a low mass and can decay only as two hadrons, if the string mass is less than the resonance mass $M_R+0.35$ GeV, (where the resonance corresponds to the flavor content of the string). We call such strings clusters, which are allowed to decay isotropically in our model. The momenta of cluster decay products are determined by the cluster mass. We would need considerable amount of data to acquire the necessary knowledge for the transverse distributions in cluster decays.

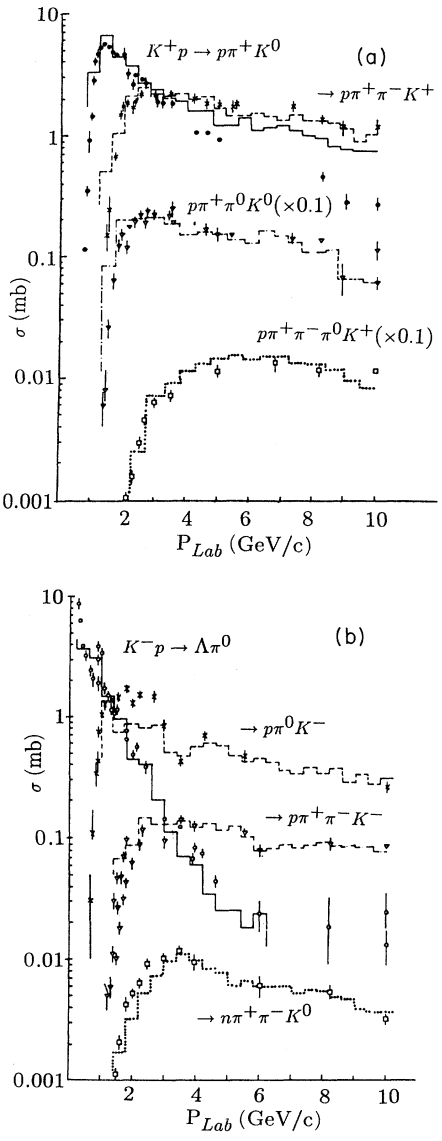

FIG. 1. Partial cross sections of different subprocesses, as a function of the K^+ projectile momentum, in $K^{\pm}p$ interactions computed with the QGSM (histograms) and compared to experimental data [29]. Labels from top to bottom: (a) solid line, $K^+p \rightarrow p\pi^+K^0$; dashed line, $K^+p \rightarrow p\pi^+\pi^-K^+$; dot-dashed line, $K^+p \rightarrow p\pi^+\pi^0K^0$; dotted line, $K^+p \rightarrow p\pi^+\pi^-\pi^0K^+$; (b) solid line, $K^-p \rightarrow \Lambda\pi^0$; dashed line, $K^-p \rightarrow p\pi^0K^-$; dot-dashed line, $K^-p \rightarrow p\pi^+\pi^-K^-$; dotted line, $K^-p \rightarrow n\pi^+\pi^-K^0$.

III. COMPARISON TO EXPERIMENTS

The QGSM provides a tool to predict rapidity and p_t distributions for strange (and nonstrange) mesons and baryons,

It should be mentioned that in Ref. [24] an explanation of K^+ enhancement without the QGP scenario was suggested by an analysis of p_t spectra with the RQMD model. However, the calculated spectra were shown only for the experimental [19] range and without absolute normalization. In a recent report RQMD spectra with absolute normalization show an overall (except for the proton rapidity distribution in central collisions) general agreement with the data [28].

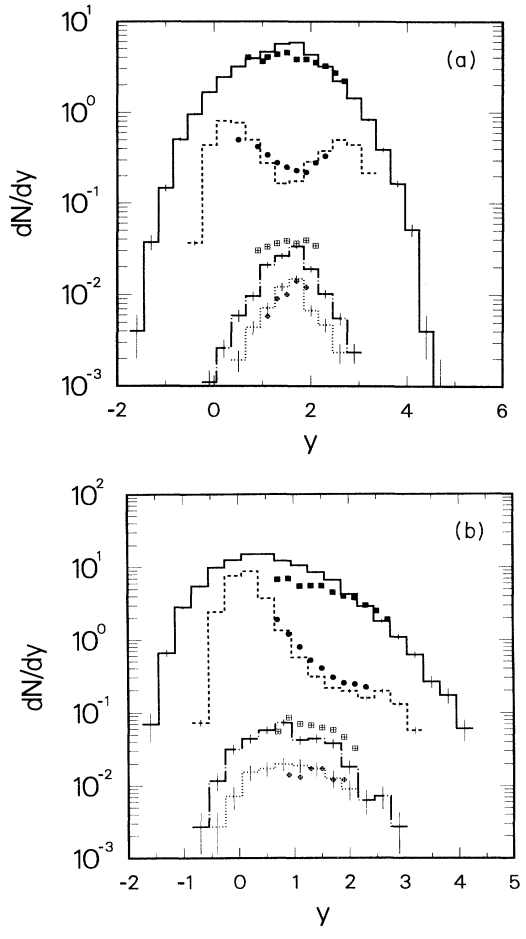

FIG. 2. Rapidity distributions dN/dy for identified particles per trigger in two different reactions (a) $p+$Be and (b) $p+$Au, at $E_{\rm lab}/A=14.6$ GeV. Different symbols are the results of E802 Collaboration [19,30,20]. Histograms are the QGSM predictions. The solid line and solid squares correspond to π^- (multiplied by 10), dashed line and solid circles to p, dot-dashed line and open squares to K^+, and dotted line and open diamonds to K^-.

A. Minimum-bias events

Rapidity distributions in the range $0.7<y<2.7$ are shown in Fig. 2 for p,π^-, and K^+ at $14.6A$ GeV for two reactions: minimum-bias $p+$Be and $p+$Au. The QGSM rapidity distributions are presented in Fig. 2 for the full rapidity range. As seen from Fig. 2, we approximately reproduced not only the shapes, but also the absolute values of dN/dy for different particles in the $p+$Be reaction. This indicates a satisfactory approximation of elementary hadron collisions. For $p+$Au we reproduced the shapes and absolute values for protons and kaons, but we overestimated the maximum values of pions. However, we also include low p_t pions, which are only extrapolated in most experiments. For lack of experimental data for pions with low transverse momentum, we cannot make a definite conclusion regarding the fit to the pion rapidity distribution.

In $p+$Be reactions the pion and kaon distributions peak nearly at the nucleon-nucleon c.m., indicating that in these reactions meson production is dominated by the initial nucleon-nucleon collisions. In the $p+$Au collisions the pion and kaon distributions peak closer to the target rapidity, at $y\approx 0.5$ and 0.8, respectively, indicating the importance of rescatterings and the approach toward equilibrium. The higher peak rapidity for kaons compared to pions shows that relatively more kaons than pions are created in initial nucleon-nucleon collisions. On the other hand, the kaon rapidity distribution is observably wider in $p+$Au, $\Delta y\approx 1.6$, than in $p+$Be, signaling that multiple scatterings influence the kaons also.

B. Central Si+Au events

1. Rapidity and transverse momentum distributions in E810

At first, we compare the QGSM predictions for rapidity distributions to E810 data because these include particles in a large transverse momentum range. In experiment E810 negative and positive particles with low transverse momenta were measured in the rapidity range $y>1.7$. We used the criteria for central Si+Au collisions that all protons except one should participate. This should be compared to the trigger condition by E810, which requires a maximum signal of $Z<1.5$ in the veto counter. The obtained rapidity spectra for negative pions and for protons are compared to experimental data [21] for negatives and positives minus negatives, respectively, in Fig. 3. We reproduce the negative-particle data at $y>2.0$, but the QGSM proton distribution disagrees substantially with the experimental results.

This indicates that our selection of events is not identical to the E810 experimental trigger condition, which will be discussed further in connection with the analyses of the E802 data.

Both the pion and kaon rapidity distributions peak around $y\approx 1$, unlike in the $p+$Au collision where there was a rapidity difference between the two peaks of about 0.3. This indicates a further increase of thermalization. The widths are about the same as in the $p+$Au case. Fluid-dynamical calculations predict a peak at $y\approx 0.8$

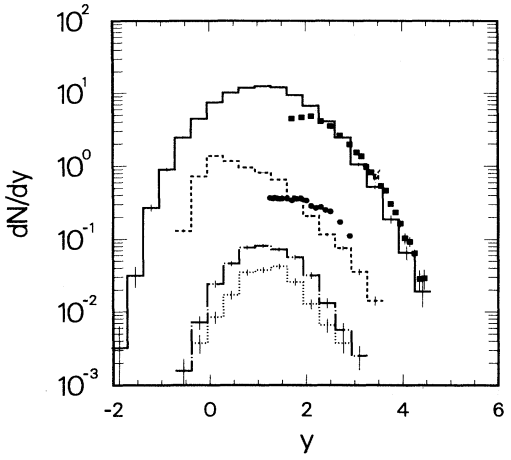

FIG. 3. Rapidity distributions dN/dy divided by 28 in central Si+Au reactions at $E_{\rm lab}/A=14.6$ GeV. Different symbols are the results of E810 Collaboration [21] for negative and positive minus negative, while the histograms are the QGSM predictions for negative pions and protons, respectively. Notation is the same as in Fig. 2.

(1.0) for hadronic (QGP) EOS's (equation of states), respectively, in a S+Pb reaction at the same energy [6]. The width and amplitude of the pion distribution are about the same in the fluid-dynamical model and QGSM. Although from the peak position one could infer the softness of the EOS [6], the sensitivity at this energy is small, and we cannot draw a definite conclusion concerning the EOS.

In Fig. 4 we present the transverse momentum spectra. Because of scaling behavior observed in pp collisions, these spectra are usually plotted as a function of the transverse mass m_t or transverse kinetic energy $T=m_t-m_0$ for a particle of mass m_0. The squares in Fig. 4 correspond to central Si+Au data for negative particles measured by E810 [21] for the rapidity interval $y=2.2-2.4$. The E810 data show a curved m_t spectrum for the Si+Au case. In Fig. 4 we present also the transverse kinetic-energy spectra for negative pions obtained by the QGSM in the same rapidity interval. As seen from Fig. 4, the main reason for the disagreement between the experimental and QGSM rapidity distributions (shown in Fig. 3) is the overprediction of the low p_t enhancement for negative particles at $T<0.2$ GeV/c.

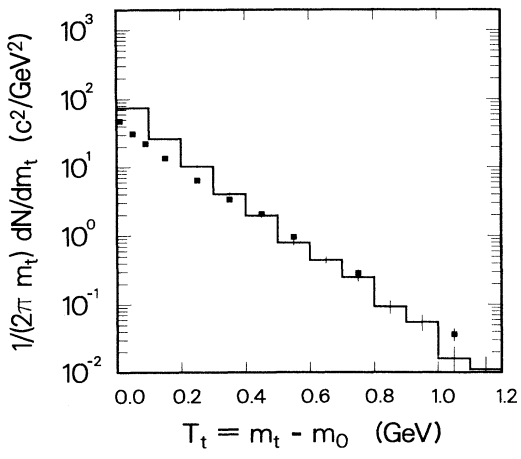

FIG. 4. Transverse mass spectra for central Si+Au collisions. The squares are measured negative particles [21] by E810 for $y=2.2-2.4$. The histogram is the result of the QGSM for π^-.

The enhancement of negatives at low p_t may be decreased by including additional collective absorption processes to the Δ resonance process ($\pi NN\rightarrow\Delta N\rightarrow NN$) mentioned in Sec. II. For example, meson absorption is possible on a correlated pair of nucleons also [25]. Furthermore, if the formation of a mean field is considered in the model, as in Ref. [23], the nuclear compression has to be realized by the use of compressional energy, which is in turn missing for meson production, leading to a lower π multiplicity.

On the other hand, in our opinion we could also decrease this disagreement by better understanding and simulation of experimental trigger conditions.

2. *Rapidity and transverse momentum distributions in E802*

Because of our lack of knowledge of the experimental conditions, we cannot reproduce the E802 central trigger as well as the E810 trigger in these simulations. Thus we performed a series of calculations at fixed impact parameters. The calculated rapidity distributions at $b=2$, 4.5, and 7 fm are shown in Fig. 5. Based on theoretical considerations, the rapidity distributions are approximately the same at impact parameters $b<3$ fm. By comparing QGSM and experimental E802 proton spectra, we conclude that central events in the experiment should roughly correspond to $b<3$ fm. The proton rapidity distribution in Fig. 5 from the E802 collaboration is substantially different from the positive-negative difference in Fig. 3. A comparison of the yields of both experiments to the theoretical impact-parameter dependence of the proton distribution from the QGSM indicates that the experiments sample events in different impact-parameter ranges. In our opinion the E810 trigger included impact parameters up to $b\sim6$ fm and cannot be represented by a simple impact parameter cut in contrast to the high centrality of the E802 result.

The E802 Collaboration concluded [19] that the K^+/π^+ ratio in central Si+Au collisions is enhanced at least by a factor of 4 as compared to pp interactions, whereas there is no clear evidence in E802 results for K^-/π^- enhancement. Experimental relative yield ratios for central Si+Au collisions [19,20] in this region are $K^+/\pi^+=0.2$ and $K^-/\pi^-=0.04$, while corresponding values in proton-proton interactions at similar energies are $K^+/\pi^+=0.5$ and $K^-/\pi^-=0.03$.

For comparison we calculated the relative yield ratios

for the QGSM in different rapidity ranges. For central Si+Au collisions at $b<5$ fm, we find $K^+/\pi^+=0.07-0.09$ and $K^-/\pi^-=0.025-0.035$, while between $b=5$ and 9 fm the K^+/π^+ ratio drops smoothly

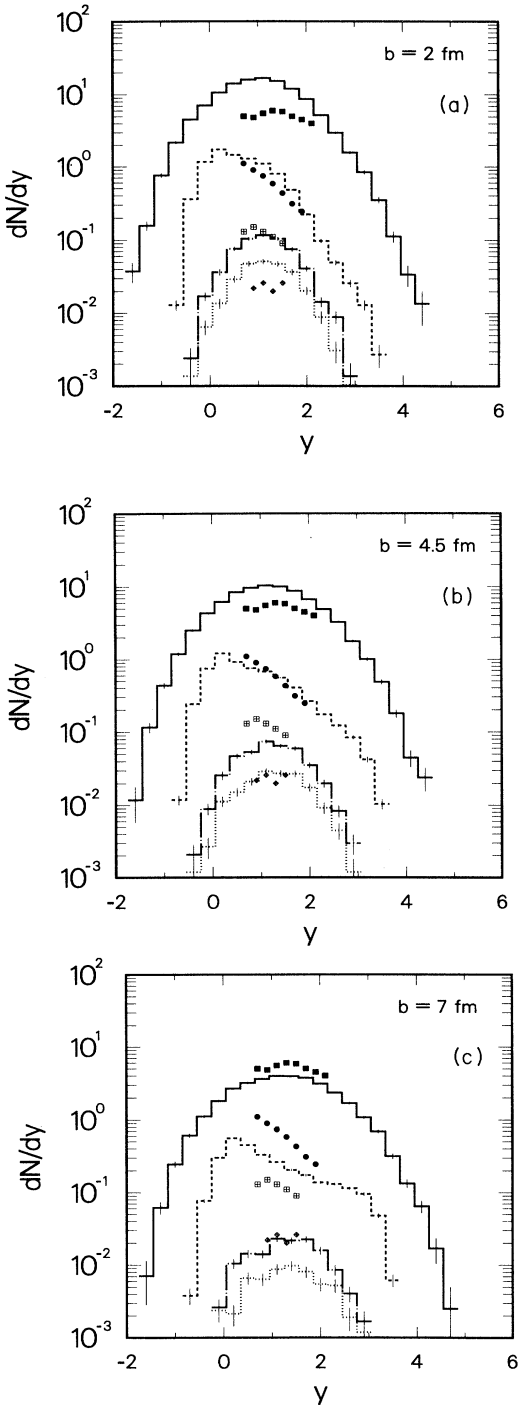

FIG. 5. Rapidity distributions dN/dy divided by 28 for identified particles in central Si+Au reactions at $E_{\rm lab}/A=14.6$ GeV at $b=$ (a) 2 fm , (b) 4.5 fm, and (c) 7 fm. Experimental data are from E802 central events [30]. Notation is the same as in Fig. 2.

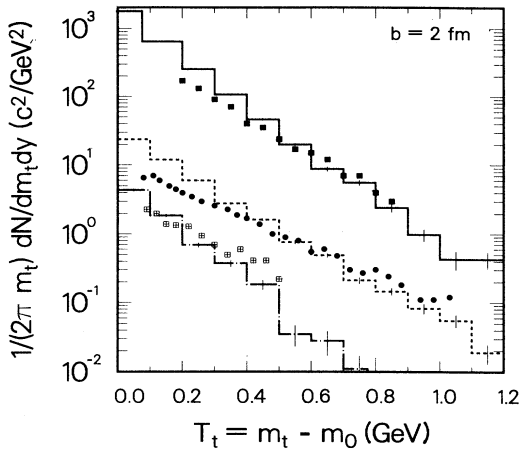

FIG. 6. Transverse mass spectra for central Si+Au collisions. Symbols correspond to data [19] from E802 measured at $y=1.2-1.4$. The histograms are results of the QGSM predictions at $b=2$ fm. Notation is the same as in Fig. 2.

to 0.04. Compared to pp collisions, this means an increase in the K^+/π^+ ratio by 1.4–1.9, but no increase for the K^-/π^- ratio.

Rapidity distributions were obtained by E802 using an exponential extrapolation to $p_t=0$. Transverse momentum spectra are measured by E802 in an interval centered at about midrapidity ($y=0.7-2.0$), and for transverse momenta $p_t>0.3$ (0.4) GeV/c for pions and kaons (protons) in a high-resolution spectrometer.

In Fig. 6 transverse mass spectra for negative pions, protons, and K^+ mesons are shown. The symbols in Fig. 6 correspond to central Si+Au data for different particles measured by E802 for the rapidity interval $y=1.2-1.4$. In Fig. 6 we present also the transverse kinetic-energy spectra (histograms) obtained by the QGSM at impact parameter $b=2$ fm. In the model low p_t spectra show a clear increase above the exponential function describing the E802 data at $p_t>0.2$ GeV/c. The low p_t enhancement is due to the long time (we followed about 30 fm/c) evolution of the hadronic system. This includes such sources of low-momentum hadrons, as the decay of resonances, mostly deltas to pions.

It should be mentioned that our model underpredicted the slope of the experimental distributions for central Si+Au. This disagreement could be resolved, if appropriate experimental $h+h$ data were available. Then, by fitting the experimental transverse momentum distributions at the hadronic level and changing model parameters accordingly, we could expect a better agreement with heavy-ion experiments also.

IV. THEORETICAL CONCLUSIONS

The QGSM gives a quantitative prediction of rapidity and transverse momentum distribution of pions, protons, and kaons for minimum-bias $p+$Be, $p+$Au, and central

Si+Au at 14.6A GeV/c in the absence of QGP. The QGSM reproduced the shapes and approximately absolute values of the minimum-bias rapidity distribution for all particles except pions in p +Au.

The QGSM gives predictions for K^+/π^+ and K^-/π^- as a function of impact parameter in Si+Au at 14.6A GeV. The model yields an enhancement of K^+ by a factor of 1.4–1.9, whereas there is no enhancement for K^-/π^-. If the QGSM K^+ yield in Fig. 5 is divided by the experimental data for negatives, the K^+/π^+ ratio gives 18%, while dividing with the QGSM pion distribution, which fits the data in the range $y > 2.0$ well, yields a ratio of 7.5%. (We assume, based on QGSM results, that the π^+ and π^- yields are identical.)

Furthermore, the QGSM overestimated the observed enhancement of the low p_t spectrum for negative-charged particles obtained by the E810 Collaboration. As a consequence, the QGSM also overestimated the rapidity distributions of negative mesons below $y = 2.0$. However, the rapidity distribution for negative mesons is reproduced by the QGSM at $y > 2.0$.

The shape of the proton rapidity distribution is strongly dependent on the impact parameter. The shoulder of the positive-negative rapidity distribution in the E810 experiment at $y = 3$ is not reproduced by the QGSM (Fig. 3). This indicates that the experiment contains events with large impact parameters (like $b > 4$ fm in Fig. 5). On the other hand, we obtained good agreement between the QGSM results for the proton distribution at $b = 2$ fm and the identified proton yield by the E802 Collaboration.

We also reproduced the experimental rapidity distribution for K^+ mesons. However, our analysis of the E802 results shows that there are still open questions about the claimed overall enhancement of K^+/π^+ ratio by a factor of 4 compared to p +p data.

The disagreements between the data and our calculations imply that description of π and K^- absorption processes should be improved in the theoretical model.

Finally, we conclude that the QGSM satisfactorily reproduces most basic features of the Si+Au data; thus there is no compelling reason to introduce QGP effects to explain K^+ production. This conclusion is in agreement with earlier fluid-dynamic estimates [6], which predicted only a negligible QGP formation (6% of the S volume) in S+Pb reactions at this energy.

ACKNOWLEDGMENTS

Valuable contributions of S. Yu. Sivoklokov and enlightening discussions with B. Müller, J. Rafelski, and H. Sorge are gratefully acknowledged. One of the authors (L.C.) is grateful for the kind hospitality of the Institute for Nuclear Theory in Seattle, where part of this work was done. This work was supported by the Norwegian Research Council for Science and Humanities.

[1] T. Abott *et al.*, Phys. Lett. B **197**, 285 (1987).
[2] M. S. Tannenbaum, *et al.*, Nucl. Phys. **A488**, 555c (1988).
[3] P. Braun-Munzinger *et al.*, Z. Phys. C **38**, 45 (1988).
[4] J. Stachel, Rapporteur's talk, PANIC XII, International Conference on Particles and Nuclei, MIT, 1990 (unpublished).
[5] J. Stachel and P. Braun-Munzinger, Phys. Lett. B **216**, 1 (1989); Nucl. Phys. **A498**, 577c (1989).
[6] E. F. Staubo, A. K. Holme, L. P. Csernai, M. Gong, and D. Strottman, Phys. Lett. B **229**, 351 (1989).
[7] T. Abbot *et al.*, Z. Phys. C **38**, 36 (1988).
[8] N. S. Amelin, K. K. Gudima, V. D. Toneev, and S. Yu. Sivoklokov, Bergen Scientific/Technical Report No. 224/1990.
[9] N. S. Amelin, E. F. Staubo, L. P. Csernai, V. D. Toneev, K. K. Gudima, and D. Strottman, Bergen Scientific/Technical Report No. 238/1990; Los Alamos report No. LA-UR-90-4305, 1990; Phys. Lett. B **261**, 352 (1991).
[10] N. S. Amelin, E. F. Staubo, L. P. Csernai, V. D. Toneev, K. K. Gudima, and D. Strottman, Bergen Scientific/Technical Report No. 240/1990; Phys. Rev. Lett. (submitted).
[11] J. Rafelski and B. Müller, Phys. Rev. Lett. **48**, 1066 (1982); **56**, 2334(E) (1986).
[12] J. Rafelski, Phys. Rep. **88**, 331 (1982).
[13] B. Müller, *The Physics of the Quark-Gluon Plasma,* Vol. 225 of *Lecture Notes in Physics* (Springer-Verlag, Berlin, 1985).
[14] P. Koch, B. Müller, and J. Rafelski, Phys. Rep. **142**, 169 (1986).
[15] N. S. Amelin and L. P. Csernai, in *Proceedings of the International Workshop on Correlations and Multiparticle Production (CAMP),* Marburg, Germany, 1990 (World Scientific, Singapore, 1990); Bergen Scientific/Technical Report No. 230/1990.
[16] N. S. Amelin, K. K. Gudima, and V. D. Toneev, Yad. Fiz. **51**, 512 (1990) [Sov. J. Nucl. Phys. **51**, 1093 (1990)].
[17] N. S. Amelin, K. K. Gudima, and V. D. Toneev, in *The Nuclear Equation of State,* Vol. 216V of *NATO Advanced Study Institute, Series B: Physics,* edited by W. Greiner and H. Stöcker (Plenum, New York, 1989), p. 473.
[18] N. S. Amelin, K. K. Gudima, S. Yu. Sivoklokov, and V. D. Toneev, Yad. Fiz. **52**, 272 (1990) [Sov. J. Nucl. Phys. **52**, 172 (1990)].
[19] T. Abbot *et al.*, Phys. Rev. Lett. **64**, 847 (1990).
[20] Y. Miake, *et al.*, E802 Collaboration, in Proceedings of "Quark Matter 90" [Nucl. Phys. **A525**, 231c (1991)].
[21] W. A. Love *et al.*, E810 Collaboration, in Proceedings of the Workshop on Heavy Ion Physics at the AGS, BNL, 1990, edited by O. Hansen (unpublished).
[22] K. Werner, Phys. Lett. B **219**, 111 (1989); K. Werner, Z. Phys. C **42**, 567c (1989).
[23] H. Sorge, H. Stöcker, and W. Greiner, Nucl. Phys. A **498**, 567c (1989).
[24] R. Matiello, H. Sorge, H. Stöcker, and W. Greiner, Phys. Rev. Lett. **63**, 1459 (1989).
[25] V. D. Toneev and K. K. Gudima, Nucl. Phys. **A400**, 173c (1983).
[26] N. S. Amelin *et al.*, Fiz. Elem. Chastits At. Yadra **13**, 130

(1982) [Sov. J. Part. Nucl. **13**, 55 (1982)].
[27] N. S. Amelin, L. B. Bravina, L. I. Sarycheva, and L. V. Smirnova, Yad. Fiz. **51**, 841 (1990) [Sov. J. Nucl. Phys. **51**, 535 (1990)].
[28] H. Sorge, R. Matiello, A. Jahns, H. Stöcker, and W. Greiner, Phys. Lett. (in press).
[29] V. Flaminio *et al.*, Report No. CERN-HERA 84-01, 1984.
[30] T. Abbot *et al.*, Phys. Rev. Lett. **66**, 1567 (1991).